

1 **Position Effects Influencing Intrachromosomal Repair of a Double-Strand Break**
2 **in Budding Yeast**

3

4 Ruoxi W. Wang¹, Cheng-Sheng Lee², and James E. Haber*

5 Department of Biology and Rosenstiel Basic Medical Sciences Research Center

6 Brandeis University

7 Waltham, MA 02454-9110

8

9

10 1 current address: Department of Biology, Massachusetts Institute of Technology,
11 Cambridge, MA 02139

12 2 current address: Department of Genetics, Harvard Medical School, Boston, MA
13 02115

14

15 * To whom correspondence should be addressed: haber@brandeis.edu

16

17 **Running Title: Intrachromosomal Recombination in Budding Yeast**

18 **Abstract**

19 Repair of a double-strand break (DSB) by an ectopic homologous donor sequence is
20 subject to the three-dimensional arrangement of chromosomes in the nucleus of haploid
21 budding yeast. The data for interchromosomal recombination suggest that searching
22 for homology is accomplished by a random collision process, strongly influenced by the
23 contact probability of the donor and recipient sequences. Here we explore how
24 recombination occurs on the same chromosome and whether there are additional
25 constraints imposed on repair. Specifically, we examined how intrachromosomal repair
26 is affected by the location of the donor sequence along the 812-kb chromosome 2
27 (Chr2), with a site-specific DSB created on the right arm (position 625kb). Repair
28 correlates well with contact frequencies determined by chromosome conformation
29 capture-based studies ($r = 0.85$). Moreover, there is a profound constraint imposed by
30 the anchoring of the centromere (*CEN2*, position 238kb) to the spindle pole body.
31 Sequences at the same distance on either side of *CEN2* are equivalently constrained in
32 recombining with a DSB located more distally on one arm, suggesting that sequences
33 on the opposite arm from the DSB are not otherwise constrained in their interaction with
34 the DSB. The centromere constraint can be partially relieved by inducing transcription
35 through the centromere to inactivate *CEN2* tethering. In diploid cells, repair of a DSB
36 via its allelic donor is strongly influenced by the presence and the position of an ectopic
37 intrachromosomal donor.

38

39 **Author Summary**

40 A double-strand break (DSB) on a chromosome can be repaired by recombining with an
41 ectopic homologous donor sequence. Interchromosomal ectopic recombination is
42 strongly influenced by the three-dimensional arrangement of chromosomes in the
43 nucleus of haploid budding yeast, that is strongly influenced by the probability of
44 chemical cross-linking of the donor and recipient sequences. Here we explore how
45 recombination occurs on the same chromosome. We examined how intrachromosomal
46 repair is affected by the location of the donor sequence along the 812-kb chromosome 2
47 (Chr2), with a site-specific DSB created on the right arm (position 625kb). Repair
48 correlates well with contact frequencies determined by chromosome conformation
49 capture-based studies ($r = 0.85$). Moreover, there is a profound constraint imposed by
50 the anchoring of the centromere (*CEN2*, position 238kb) to the spindle pole body.
51 Sequences at the same distance on either side of *CEN2* are equivalently accessible in
52 recombining with a DSB located more distally on one arm, suggesting that sequences
53 on the opposite arm from the DSB are not otherwise constrained in their interaction with
54 the DSB. The centromere constraint can be partially relieved by inducing transcription
55 through the centromere to inactivate *CEN2* tethering. In diploid cells, repair of a DSB
56 via its allelic donor is strongly influenced by the presence and the position of an ectopic
57 intrachromosomal donor.

58

59

60

61 **Introduction**

62 A fundamentally important step in the repair of a broken chromosome by
63 homologous recombination is the identification and use of a homologous donor
64 sequence to repair the DSB [Agmon, 2013 #12545;Lee, 2016 #12798;Inbar, 1999
65 #10663;Haber, 2013 #11987;Coic, 2011 #10624;Lichten, 1989 #643](1–6). In
66 eukaryotes, DSBs are processed by exonucleases to expose 3'-ended single-stranded
67 regions upon which Rad51 recombination protein is loaded and forms a nucleoprotein
68 filament. The Rad51 filament, like its bacterial RecA counterpart, then interrogates
69 other sequences in the genome to locate a homologous segment with which it can
70 promote strand invasion to form a displacement loop and then initiate DNA synthesis
71 using the homologous sequence as a template to repair the DSB. How the search for
72 homology – on a sister chromatid, a homologous chromosome or at an ectopic site –is
73 accomplished remains a subject of active investigation. Several lines of evidence
74 suggest that the search is more efficient intrachromosomally – at least over modest
75 distances of 100- 200 kb [Lichten, 1989 #643;Lee, 2016 #12798](2,6), but this question
76 needs to be explored in more detail.

77 Recently we developed an ectopic donor assay to study DSB repair efficiency in
78 haploid *Saccharomyces cerevisiae* [Lee, 2016 #12798](2). A site-specific DSB, created
79 by the galactose-inducible HO endonuclease, could be repaired by a single ectopic
80 donor sequence, which shares 1 kb homology with either side of the break and is
81 located elsewhere in the genome. By placing a donor at 20 different locations
82 throughout the genome, we showed that the efficiency of interchromosomal
83 recombination was strongly correlated with the likelihood that the donor region would

84 come into contact with the recipient site, based on chromosome conformation capture
85 analysis [Duan, 2010 #10805; Lee, 2016 #12798](2,7). In some cases, a donor site that
86 was quite inefficient when used to repair the DSB on Chr5 became much more efficient
87 when confronted with a different DSB induced on Chr2, consistent with the differences
88 in its contact frequencies with the regions surrounding the two break sites. Studies by
89 Agmon et al. [Agmon, 2013 #12545](1) and by Zimmer et al. [Zimmer, 2011 #12012] (8)
90 also reached similar conclusions, with focus on the recombination when both DSB and
91 donor are located at pericentromeric or subtelomeric regions.

92 Here we have extended our analysis to examine the correlation between contact
93 frequencies and repair for intrachromosomal events. We find again a strong correlation
94 with contact frequency but also see additional constraints imposed by the centromere
95 and by the very high level of contacts made by nearby intrachromosomal sequences.

96

97 **Results**

98 **Intrachromosomal GC is subjected to chromosome organization**

99 In our previous study, we mainly focused on the correlation between
100 chromosome organization and recombination frequencies in interchromosomal
101 noncrossover gene conversion events [Lee, 2016 #12798] (2). A DSB was induced
102 within *leu2* sequences inserted on Chr5, while a homologous 2-kb *LEU2* donor was
103 placed at 4 positions on the same chromosome or at 20 locations on different
104 chromosomes. Repair occurs predominantly by synthesis-dependent strand annealing
105 in which by a patch of DNA newly copied from the donor to replaces the 117-bp HO
106 cleavage site sequences [Lee, 2016 #12798][Ira, 2006 #2857] (2,9). We and others

107 have observed that intrachromosomal gene conversion occurred generally more
108 efficiently and with a faster kinetics than interchromosomal events [Lee, 2016
109 #12798; Agmon, 2013 #12545][Mehta, 2017 #13041] (1,2,10).

110 To examine intrachromosomal repair in more detail, we constructed a series of
111 12 strains, in which a DSB was created within a 2-kb *LEU2* gene inserted 625kb from
112 the left end on chromosome 2 (Chr2) and a donor was inserted at different sites across
113 the chromosome (Figure 1A). The DSB, created by galactose-inducible expression of
114 the HO endonuclease gene, is situated 387 kb from *CEN2* and 187 kb from the right
115 telomere (<http://www.yeastgenome.org/>). The efficiency of DSB repair of each of the 12
116 strains was measured by plating cells on YEP-galactose plates to continuously induce
117 the HO endonuclease, compared to the same number of cells plated on glucose-
118 containing medium. Virtually all of the survivors repaired the DSB by ectopic gene
119 conversion rather than by nonhomologous end-joining, which occurs only in 0.2% of
120 cases [Lee, 2016 #12798](2). Cell viabilities among the 12 strains ranged from 9% to
121 89%; because these repair events occur on the first cell cycle, the observed frequencies
122 are equivalent to rates.

123 Repair efficiencies were then plotted with respect to the total contact frequencies
124 between the DSB region and the donor region, which is calculated by adding up all the
125 interaction reads, measured by [Duan, 2010 #10805] (7), between +/-25kb region
126 surrounding the DSB site and either a +/-10kb (Figure 1B) or +/-20kb (Figure 1C) region
127 surrounding a donor site. Cell viability displayed a strong correlation with the total
128 contact frequency; however, the effect of contact frequency on cell viability approached
129 saturation when donor was within about 100 kb of the DSB, where contact frequencies

130 also reached a maximum (Figure S1B). The calculated correlation coefficient using
131 Pearson correlation analysis was $r = 0.82$ ($P = 2 \times 10^{-3}$) with +/-10kb window around the
132 donor and $r = 0.85$ ($P = 5 \times 10^{-4}$) with +/-20kb window around the donor. Thus,
133 intrachromosomal recombination is strongly constrained by the likelihood that two
134 sequences will come into contact, as we saw for interchromosomal events.

135 We note that when donors were located within 50 kb from a telomere (locus 1
136 and 12), their measured viabilities were higher than expected based on their contact
137 frequency (Figure 1B and 1C). It has been reported that chromosomal conformation
138 capture methods tend to underestimate productive contacts in subtelomeric regions
139 [Duan, 2010 #10805] (7). Although sequences more than 20 kb from a telomeric
140 anchor appear to be unconstrained [Avsaroglu, 2014 #12111] (11), it seems possible
141 that the underestimation of contact frequencies may explain the higher-than-predicted
142 recombination efficiencies for these two loci. The results for donors placed within 100
143 kb of the DSB target appear to reflect a plateau, consistent with the leveling off of
144 contact frequencies (Figure S1B).

145

146 **DSB repair is constrained by centromere tethering**

147 If one plots the correlation between cell viability and the distance of a
148 homologous *LEU2* donor from the left end of Chr2, it becomes evident that donors
149 located close to the centromere display a low repair rate compared to donors located
150 within a chromosome arm (Figure 2A). Indeed, the efficiencies of repair are in
151 agreement with the idea that the two chromosome arms are in the Rabl orientation [Jin,
152 2000 #137] (12), with the centromere anchored at the spindle pole body (SPB) (Figure

153 S1A). In budding yeast the centromere remains attached to the SPB throughout the cell
154 cycle [Tanaka, 2007 #147] (13). Interestingly, if one re-plots recombination efficiencies
155 as a function of the distance from *CEN2*, it becomes apparent that the left arm – where
156 the homologous *LEU2* locations are significantly more linearly distant from the DSB
157 itself – behaves as if these sites are as accessible as those on the right arm (Figure 2B).
158 These results suggest that the tethering of the telomere of the left arm does not prevent
159 sequences from interacting with the DSB on the opposite arm as efficiently as sites on
160 the right arm, when the sites are equally distant from the centromere.

161

162 To further explore if the correlation between genomic distance and cell viability is
163 affected by centromere tethering, we enquired whether detaching the centromere from
164 SPB would alter the pattern of repair we observed in wild type strains. Cohesin is an
165 essential protein complex that facilitates spindle attachment to the centromere. Mcm21
166 is a non-essential kinetochore component of the COMA complex [Ortiz, 1999 #13034]
167 (14) that is responsible for the enrichment of cohesin at the pericentromeric region.
168 Deletion of *MCM21* results in a partial dispersal of kinetochores from the normal cluster
169 around the SPB, but does not prevent relatively normal chromosome segregation
170 [Tsabar, 2016 #12794] (15). However, deleting *MCM21* did not result in a change in
171 repair efficiency (and thus cell viability) among four of the *MCM21* deletion strains
172 whose donors were close to *CEN2* (Figure 3A), suggesting that the depletion of Mcm21
173 protein might not be sufficient to fully inactivate the attachment of centromere to the
174 SPB.

175

176 As an alternative way of disrupting kinetochore attachment to the SPB, we
177 introduced a conditionally functional centromere by placing a galactose-inducible
178 promoter upstream of the centromeric DNA sequence [Hill, 1989 #661;Tsabar, 2016
179 #12794] (15,16). A *GAL::CEN* centromere is functional when cells are grown on
180 glucose-containing plate but its function is impaired when cells are transferred to
181 galactose-containing plate, as the strong transcription disrupts normal assembly of the
182 kinetochore at this centromere. Our recent study of the *GAL-CEN3* construct showed
183 that sister chromosomes properly segregated only 1/3 of the time, and then only after
184 some delay [Tsabar, 2016 #12794] (15). We therefore replaced *CEN2* with *cen2::GAL-*
185 *CEN3* in several of the intra-chromosomal donor strains (Figure 3B). Placing cells on
186 galactose, which simultaneously induced HO endonuclease expression and inactivated
187 the Chr2 centromere, had no significant effect on donors located far from *CEN2*, but did
188 significantly raise the level of repair of two loci near *CEN2* (Figure 3C).

189
190 To confirm that transcription did indeed perturb centromere function in these
191 strains we carried out pedigree analysis to measure missegregation of the chromosome
192 by the appearance of daughter cells that failed to inherit Chr2 [Tsabar, 2016 #12794]
193 (15). To be sure that segregation was not also influenced by the HO cleavage, we
194 modified strains by removing the HO cleavage site, so that only the *GAL::CEN* would be
195 affected by addition of galactose. This was accomplished by transforming the strain
196 with a *HPH*-marked plasmid expressing both Cas9 and a guide RNA targeted to the HO
197 cleavage site. Transformants grown on glucose medium proved to have lost the
198 cleavage site, by DSB-induced gene conversion using the ectopic *LEU2* donor (data not

199 shown). For strains with wild type *CEN2* (cutsite-deleted derivatives of strains YWW113
200 and 119), both mother and daughter cells gave rise to colonies in each of 45 cases. For
201 the modified strain YWW216 (donor at 220 kb, 18 kb from *CEN2*), lacking the HO
202 cutsite, 16 of 29 daughters failed to produce colonies, and for modified strain YWW231
203 (donor at 252 kb, 14 kb from *CEN2*), 7 out of 20 daughter cells failed to give rise to
204 colonies. Finding approximately 1/3 of pedigrees failing to properly disjoin the
205 *GAL::CEN* chromosome is consistent with our previous study and confirms that when
206 galactose was added to induce HO it also would disrupt normal *CEN* function [Tsabar,
207 2016 #12794] (15).

208

209 **Interchromosomal versus intrachromosomal repair of a DSB**

210 In diploid yeast, mitotic homologous chromosomes are not evidently paired with
211 each other although some preferential interactions have been reported [Burgess, 1999
212 #1589; Burgess, 1999 #1590; Lorenz, 2003 #13038] (17–19). We created diploids to ask
213 how the presence of a competing allelic donor would affect repair via an
214 intrachromosomal site. Whereas the ectopic intrachromosomal donor shares only 1 kb
215 on each side of the DSB, the homologous chromosome shares the entire chromosome
216 arm. The diploid strains were constructed by mating strains that carried the *leu2::HOcs*
217 at 625kb and an intrachromosomal ectopic *LEU2* donor at different locations with a
218 strain carrying a *URA3* selectable marker and a *leu2-K* donor at 625 kb; that is, at the
219 allelic position to the DSB (Figure 4A). Normal *MAT* sequences were deleted (see
220 Materials and Methods). In these strains, viability was nearly 100% as expected for a
221 diploid where an unrepaired DSB and chromosome loss would still lead to a viable

222 aneuploidy [Malkova, 1996 #333] (20). We assessed the use of the intrachromosomal
223 ectopic (*LEU2*) and allelic (*leu2-K*) donors by PCR-amplifying the repaired locus
224 followed by *KpnI* digestion, both in pools of cells (Figure S2) and from colonies of
225 individual recombinants (Figure 4B). HO cleavage is nearly 100% efficient so no
226 amplification occurs from the unrepaired *leu2::HOcs* site.

227 The use of the ectopic (*KpnI*⁺) donor was substantially reduced in each of three
228 examples (Figure S2C), as compared to the use measured in a haploid strain by a
229 viability assay (Figure 1B). In pooled cells, for example, for site 2 (122kb), which was
230 36.3% viable in the haploid strain assay, only 12.3% of the repair events used this
231 intrachromosomal donor. For site 8 (532kb), which was a highly efficient donor (84.7%)
232 in the haploid assay, its use was decreased to 57.7% in the diploid, with the remainder
233 coming from the allelic locus. The PCR-*KpnI* assay used in Figure S2 slightly
234 underestimates the use of the allelic donor because it fails to capture the fraction of
235 allelic gene conversion events that co-convert *leu2-K* and the adjacent *URA3* marker
236 (as illustrated in Figure 4B, bottom panel). This larger insertion was not amplified under
237 the PCR conditions used to assay the population of recombinants, as shown in Figure
238 S2B. To assess the proportion of the three types of possible outcomes, we analyzed
239 individual repair events (Figure 4B), where we used PCR conditions that recover all of
240 the relevant products. Of 31 events, 16 (51.6%) used the intrachromosomal donor,
241 while 12 repaired the DSB without co-converting the adjacent *URA3* marker and 3 co-
242 converted *URA3* along with *leu2-K*.

243

244 The ectopic donor shares 1 kb homology on either side of the DSB whereas the
245 allelic donor has extensive homology on both sides of the break (with a 1-kb insertion
246 on one side). Previously we have shown that increasing homology from 1 kb to 2 or 3
247 kb on each side of the DSB had a very significant effect on the efficiency of ectopic DSB
248 repair [Lee, 2016 #12798] (2); the data here are consistent with the idea that sharing
249 more extensive homology, even if interrupted on one side by a heterology, has a highly
250 significant effect on the likelihood that a donor will be successful in repairing the DSB;
251 but the intrachromosomal site remained the preferred donor.

252

253 **Discussion**

254 In haploid yeast genome, the sixteen chromosomes adopt a preferential 3D
255 conformation with centromeres clustered at spindle pole body and telomeres loosely
256 associated at the nuclear envelope, the so-called Rab1 configuration [Taddei, 2010
257 #13040] (21). Our previous work and that of others have shown that 3D nuclear
258 architecture is a key factor that influences the rate and efficiency of interchromosomal
259 DSB repair, with a striking correlation between repair and the estimation of the physical
260 distance of two DNA fragments in the genome (contact frequency). These studies also
261 demonstrated that a site that served as an efficient donor to repair a DSB at one
262 location could be a very inefficient donor when the site of DSB (with the same
263 homologous sequences) was moved to a different chromosome; thus most donor sites
264 were not “hot” or “cold” because of local chromatin features.

265 Here we show that chromosome conformation capture data also provide strong
266 predictions for intrachromosomal DSB repair frequencies. Sites within approximately

267 100 kb of the DSB, which show very high levels of contact frequency, reach a plateau in
268 their ability to recombine, but beyond that distance repair roughly diminishes with
269 distance as the donors are placed closer to the centromere. However, at increasing
270 distance from the centromere on the opposite chromosome arm, repair frequencies
271 increase. This pattern is consistent with the Rabl configuration of chromosomes and,
272 further, that a site 200 kb on the left arm is approximately as able to recombine as one
273 on the right arm, despite being much further away as viewed along the chromosome
274 itself. These results suggest that the left arm is not tethered away from the DSB site.
275 The high level of accessibility of sites on the left arm that are distant from the
276 centromere is not evident in the Hi-C data, which is swamped by interactions close to
277 the site of interest (Figure S1B).

278 Our results demonstrate a strong constraint on the ability of centromere-proximal
279 sequences to recombine with distant loci, although Agmon et al. [Agmon, 2013 #12545]
280 (1) showed that recombination between centromere-adjacent sequences on different
281 chromosomes is efficient, consistent with the bundling of centromere-adjacent
282 sequences held by the cluster of centromeres at the SPB. Our results contrast with
283 those of Agmon et al., who suggested that recombination involving one interstitial
284 element should not be constrained by any tethering effects.

285 Despite reports that deletion of *MCM21* leads to the partial dislocation of
286 centromeres from the SPB [Ortiz, 1999 #13034] (14), this deletion did not relieve the
287 constraint of centromere proximity in DSB repair. However, disruption of *CEN2* function
288 by galactose-induced transcription proved to cause a modest but statistically significant
289 increase in the ability of centromere-proximal sequences to recombine. We note that

290 even with *GAL::CEN* disruption, 2/3 of cells are able to maintain proper chromosome
291 segregation, so the effect of disrupting *GAL::CEN* would not necessarily be expected to
292 have a larger consequence.

293 Previously we had shown that there could be a strong competition between an
294 intrachromosomal donor and a competitor at an allelic site for spontaneous mitotic
295 recombination [Lichten, 1989 #643; Lee, 2016 #12798] (2,6). Here, we show that this
296 conclusion holds true for events known to be initiated by a site-specific DSB, depending
297 on the contact frequency between intrachromosomal sites. It will be interesting to
298 assess these results in more detail when contact probabilities have been determined in
299 diploid strains.

300

301

302 **Materials and Methods**

303 **Strains.** All strains were derived from YCSL305 (*ho hmlΔ::ADE1 mataΔ::hisG*
304 *hmrΔ::ADE1 leu2::KAN ade3::GAL::HO ade1 lys5 ura3-52 trp1*
305 *Chr2.625kb::leu2::HOcs*). The specific locations of the donors inserted on Chr2 and the
306 derivatives containing either *mcm21Δ* or a *GAL::CEN* replacement of *CEN2* are
307 presented in Table S1. A NAT-MX cassette amplified from pJH1513 was inserted at the
308 specific donor location and was then replaced by a TEFp-LEU2-TEFt fragment through
309 homologous recombination. Deletion of *MCM21* was accomplished by transforming
310 cells with a PCR-amplified NAT-marked deletion, copied from the yeast genome
311 knockout collection [Chu, 2008 #153]. The *URA3::GAL::CEN3* sequence was amplified
312 from pJH870 using PCR primers *cen2::GAL-CEN3 p4* and *cen2::GAL-CEN3 p5* to
313 replace the *CEN2* region. The sequences of the primers used in strain construction are
314 presented in Table S2.

315

316 Diploid strains were constructed by mating **a**-like strains (deleted for *MAT*) that carried
317 the *leu2::HOcs* at 625kb and an intrachromosomal ectopic *LEU2* donor at different
318 locations with another *MAT*-deleted strain carrying a *URA3* selectable marker and a
319 *leu2-K* donor at 625 kb (that is, at the allelic position to the DSB). Mating was
320 accomplished by transforming the second strain with a *TRP1*-marked *MAT α* plasmid,
321 which was not retained after mating.

322

323 **Growth conditions.** Single colonies were inoculated into YP-Lactate medium and
324 grew to log phase at 30 °C. Viability assays were carried out as described by Lee et al.
325 [Lee, 2016 #12798]. The viability was calculated as the number of colonies that grew on
326 YEP-galactose medium divided by the number of cells grew on YEPD medium. Three
327 biological replicates were performed on each strain. Pearson's correlation test was
328 conducted between viability and contact frequency.

329

330

331 **Pedigree analysis.** The disruption of normal Chr2 segregation in the *cen2::GAL::CEN3*
332 strain was determined by pedigree analysis as previously described. Individual
333 unbudded (G1) cells were micromanipulated and allowed to grow until mother and
334 daughter cells could be separated. The subsequent growth of the mothers and
335 daughters was observed after 24 h. Daughter cells that failed to inherit Chr2 at the first
336 cell division failed to proliferate beyond another cell division, whereas a normal cell or a
337 mother cell that inherited an extra copy of Chr2 grew into a microcolony.

338

339 **PCR analysis for diploid strains.** Single colonies were inoculated into 4ml of YP-
340 Lactate medium and grew at 30 °C overnight. The culture was diluted and grew to log
341 phase. Then DSB was induced by adding 20% galactose to a final concentration of 2%.
342 The repaired region was amplified from purified genomic DNA using flanking primers
343 *Mcm7p3* and *Leu2p18B* (sequences are presented in Table S2). Short PCR extension
344 time was used to avoid the amplification of *URA3* from the homologous chromosome.
345 The PCR amplicon was digested with *KpnI* overnight. The digested fragments were
346 separated and visualized on agarose gel. The relative usage of intrachromosomal

347 donors was calculated by dividing the sum of intensity of the *Kpnl* fragments by the total
348 intensity of all amplicons. The experiments were repeated for three times in each strain.

349

350 References

351

352 1. Agmon N, Liefshitz B, Zimmer C, Fabre E, Kupiec M. Effect of nuclear architecture
353 on the efficiency of double-strand break repair. *Nat Cell Biol.* 2013 Jun;15(6):694–
354 9.

355 2. Lee C-S, Wang RW, Chang H-H, Capurso D, Segal MR, Haber JE. Chromosome
356 position determines the success of double-strand break repair. *PNAS.* 2016 Jan
357 12;113(2):E146–54.

358 3. Inbar O, Kupiec M. Homology search and choice of homologous partner during
359 mitotic recombination. *Mol Cell Biol.* 1999 Jun;19(6):4134–42.

360 4. Haber J. *Genome Stability: DNA Repair and Recombination.* 1 edition. New York:
361 Garland Science; 2013. 396 p.

362 5. Coïc E, Martin J, Ryu T, Tay SY, Kondev J, Haber JE. Dynamics of Homology
363 Searching During Gene Conversion in *Saccharomyces cerevisiae* Revealed by
364 Donor Competition. *Genetics.* 2011 Dec;189(4):1225–33.

365 6. Lichten M, Haber JE. Position Effects in Ectopic and Allelic Mitotic Recombination
366 in *Saccharomyces Cerevisiae*. *Genetics.* 1989 Oct;123(2):261–8.

367 7. Duan Z, Andronescu M, Schutz K, McIlwain S, Kim YJ, Lee C, et al. A Three-
368 Dimensional Model of the Yeast Genome. *Nature.* 2010 May 20;465(7296):363–7.

369 8. Zimmer C, Fabre E. Principles of chromosomal organization: lessons from yeast. *J*
370 *Cell Biol.* 2011 Mar 7;192(5):723–33.

371 9. Ira G, Satory D, Haber JE. Conservative Inheritance of Newly Synthesized DNA in
372 Double-Strand Break-Induced Gene Conversion. *Mol Cell Biol.* 2006
373 Dec;26(24):9424–9.

374 10. Mehta A, Beach A, Haber JE. Homology Requirements and Competition between
375 Gene Conversion and Break-Induced Replication during Double-Strand Break
376 Repair. *Mol Cell.* 2017 Feb 2;65(3):515–26.e3.

377 11. Avşaroğlu B, Bronk G, Gordon-Messer S, Ham J, Bressan DA, Haber JE, et al.
378 Effect of Chromosome Tethering on Nuclear Organization in Yeast. *PLoS One*
379 [Internet]. 2014 Jul 14 [cited 2015 Dec 10];9(7). Available from:
380 <http://www.ncbi.nlm.nih.gov/pmc/articles/PMC4096926/>

- 381 12. Jin QW, Fuchs J, Loidl J. Centromere clustering is a major determinant of yeast
382 interphase nuclear organization. *J Cell Sci.* 2000 Jun;113 (Pt 11):1903–12.
- 383 13. Tanaka K, Kitamura E, Kitamura Y, Tanaka TU. Molecular mechanisms of
384 microtubule-dependent kinetochore transport toward spindle poles. *J Cell Biol.*
385 2007 Jul 16;178(2):269–81.
- 386 14. Ortiz J, Stemmann O, Rank S, Lechner J. A putative protein complex consisting of
387 Ctf19, Mcm21, and Okp1 represents a missing link in the budding yeast
388 kinetochore. *Genes Dev.* 1999 May 1;13(9):1140–55.
- 389 15. Tsabar M, Haase J, Harrison B, Snider CE, Eldridge B, Kaminsky L, et al. A
390 Cohesin-Based Partitioning Mechanism Revealed upon Transcriptional Inactivation
391 of Centromere. *PLoS Genet* [Internet]. 2016 Apr 29 [cited 2016 Dec 24];12(4).
392 Available from: <http://www.ncbi.nlm.nih.gov/pmc/articles/PMC4851351/>
- 393 16. Hill A, Bloom K. Acquisition and processing of a conditional dicentric chromosome
394 in *Saccharomyces cerevisiae*. *Mol Cell Biol.* 1989 Mar;9(3):1368–70.
- 395 17. Burgess SM, Kleckner N. Collisions between yeast chromosomal loci in vivo are
396 governed by three layers of organization. *Genes Dev.* 1999 Jul 15;13(14):1871–83.
- 397 18. Burgess SM, Kleckner N, Weiner BM. Somatic pairing of homologs in budding
398 yeast: existence and modulation. *Genes Dev.* 1999 Jun 15;13(12):1627–41.
- 399 19. Lorenz A, Fuchs J, Bürger R, Loidl J. Chromosome pairing does not contribute to
400 nuclear architecture in vegetative yeast cells. *Eukaryotic Cell.* 2003 Oct;2(5):856–
401 66.
- 402 20. Malkova A, Ivanov EL, Haber JE. Double-strand break repair in the absence of
403 RAD51 in yeast: a possible role for break-induced DNA replication. *Proc Natl Acad*
404 *Sci USA.* 1996 Jul 9;93(14):7131–6.
- 405 21. Taddei A, Schober H, Gasser SM. The Budding Yeast Nucleus. *Cold Spring Harb*
406 *Perspect Biol* [Internet]. 2010 Aug [cited 2015 Dec 11];2(8). Available from:
407 <http://www.ncbi.nlm.nih.gov/pmc/articles/PMC2908769/>

408
409
410

411 Figure Captions

412

413 Figure 1: Viability assay to assess repair efficiency for 12 intrachromosomal loci. (A)
414 The scheme of viability assay. The *leu2::HOcs* was inserted at 625 kb on Chr2. The
415 DSB could be repaired by an ectopic *LEU2* donor inserted on the same chromosome.
416 The locations for the 12 donors were shown along Chr2. (B and C) Correlation between
417 cell viability (%), shown in blue) and total contact frequency using ± 25 kb window size
418 around Chr2-DSB and ± 10 kb(B) or ± 20 kb window size around donor(C). Only 11 loci
419 were analyzed in (B) since no productive contact was detected between ± 25 kb around
420 DSB and ± 10 kb around site 4. Error bars indicate one SD from three independent
421 experiments.

422

423 Figure S1: (A) Rab1 configuration of a chromosome in budding yeast. The centromere is
424 tethered to the spindle pole body and the telomeres are clustered at the nuclear
425 envelope. (B) Distribution of intrachromosomal contacts to the DSB site (Chr2, 625kb)
426 using ± 25 kb window size around the DSB. The contact frequency between the DSB
427 and the donor is determined by adding up all individual contacts around the donor
428 location. The position of the HO cleavage site is given by a red arrow.

429

430 Figure 2: Correlation between cell viability and distance of a homologous *LEU2* donor
431 from (A) the left telomere and (B) the centromere (*CEN2*). Pearson's correlation test
432 were conducted for either side of *CEN2* (including *CEN2*) respectively. Donor sites 10-
433 12 (729kb, 742kb and 768kb) are excluded from the analysis because viability had
434 reached a plateau. $r = 0.93$ for right side of *CEN2*, and $r = 0.95$ for left side of *CEN2*.

435

436 Figure 3: (A) Effect of *mcm21 Δ* on viability. (B and C) Effect of *cen2 Δ ::GAL-CEN3* on
437 viability. Inactivation of *CEN2* significantly increased viability of two donors located close
438 to *CEN2*. Error bars indicate one SD from three independent experiments.

439

440 Figure 4: (A) Scheme for DSB repair in diploid strains. The DSB could be repaired by
441 gene conversion using an ectopic intrachromosomal *LEU2* sequence, an allelic *leu2-*

442 KpnI sequence, or the homologous sequence outside of the *leu2*-KpnI. (B) Usage of
443 ectopic and allelic donors assessed from 31 colonies of individual recombinants.

444

445 Figure S2: (A) Usage of ectopic and allelic donors assessed from a population of cells.
446 The 3kb *URA3-leu2-KpnI* sequence was excluded in the PCR-based analysis by using
447 short amplification times, as indicated by smaller arrowheads. (B) An example of donor
448 usage measurement on agarose gel (YWW210, 57.5% intrachromosomal donor usage).
449 The top band (1045bp) represents *leu2-KpnI* repair product. The lower two bands
450 (732bp and 313bp), digested by *KpnI*, represent *LEU2* repair product. The
451 intrachromosomal donor relative usage (%) was calculated as the intensity of the sum of
452 lower two bands divided by the total intensities of the three bands. (C) Plot of
453 intrachromosomal donor relative usage versus contact frequency (± 10 kb around donor
454 and ± 25 kb around DSB). The intrachromosomal donor locations and their
455 corresponding viabilities (%) in haploid strains are shown in blue. Error bars indicate
456 one SD from three independent experiments.

457

458

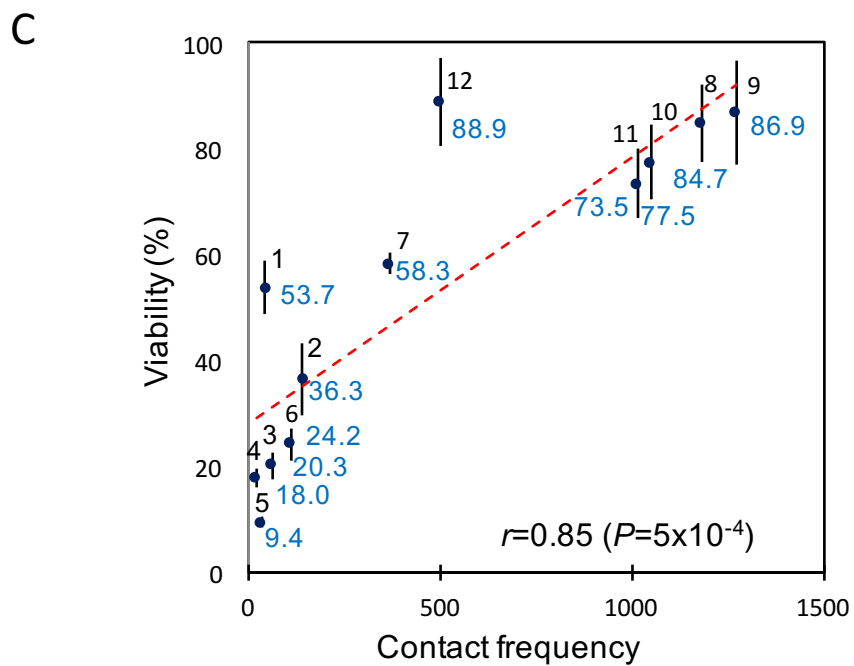
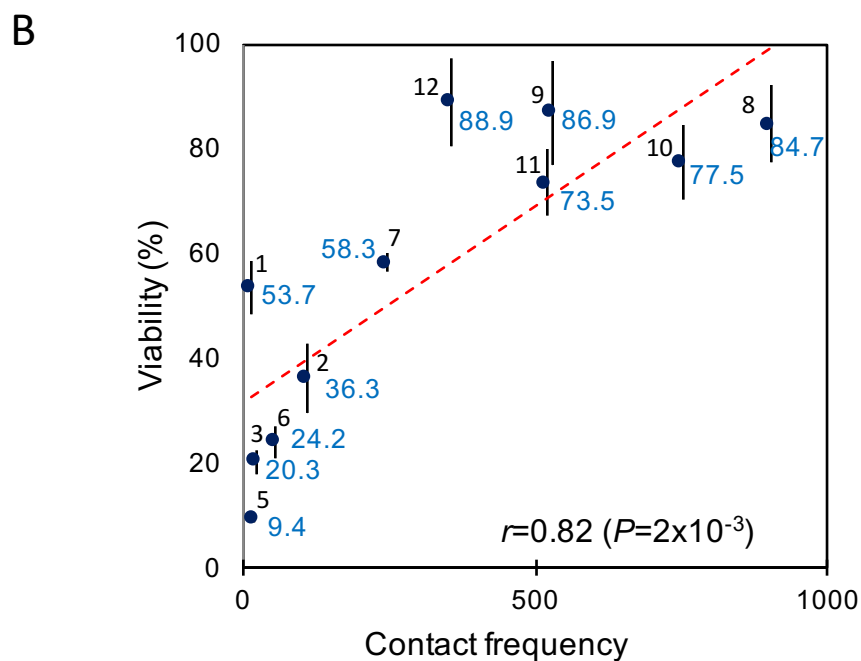
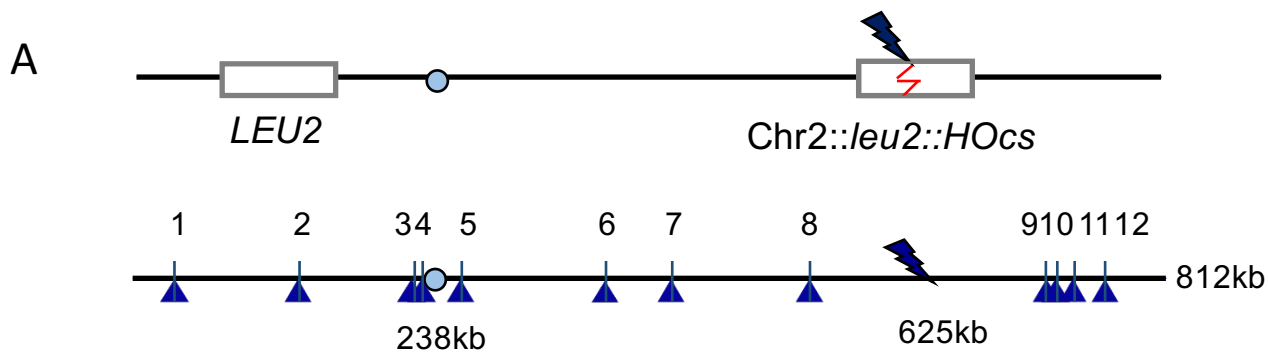


Figure 1

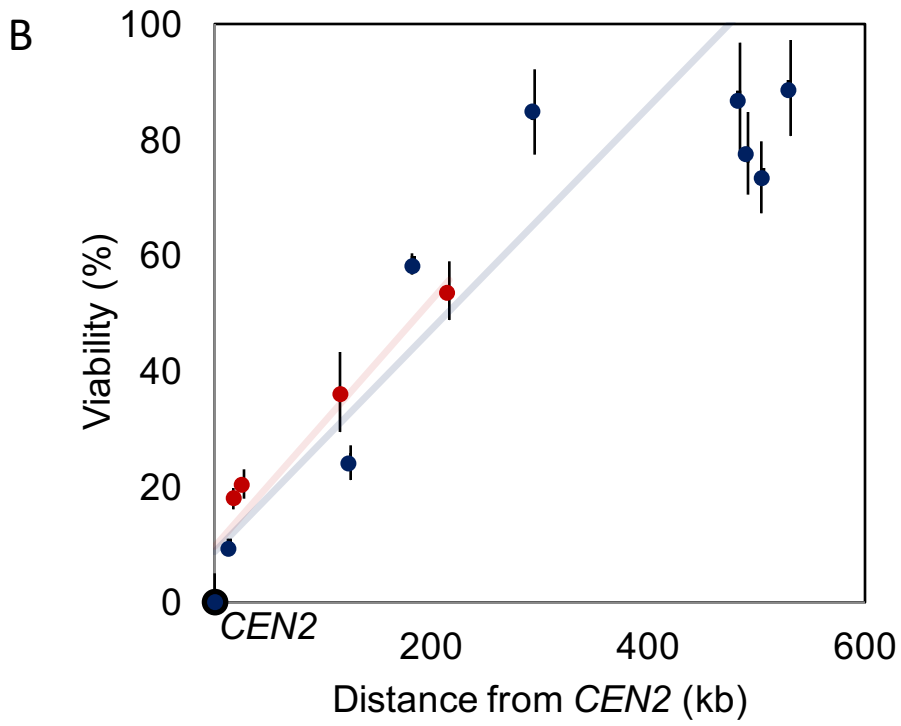
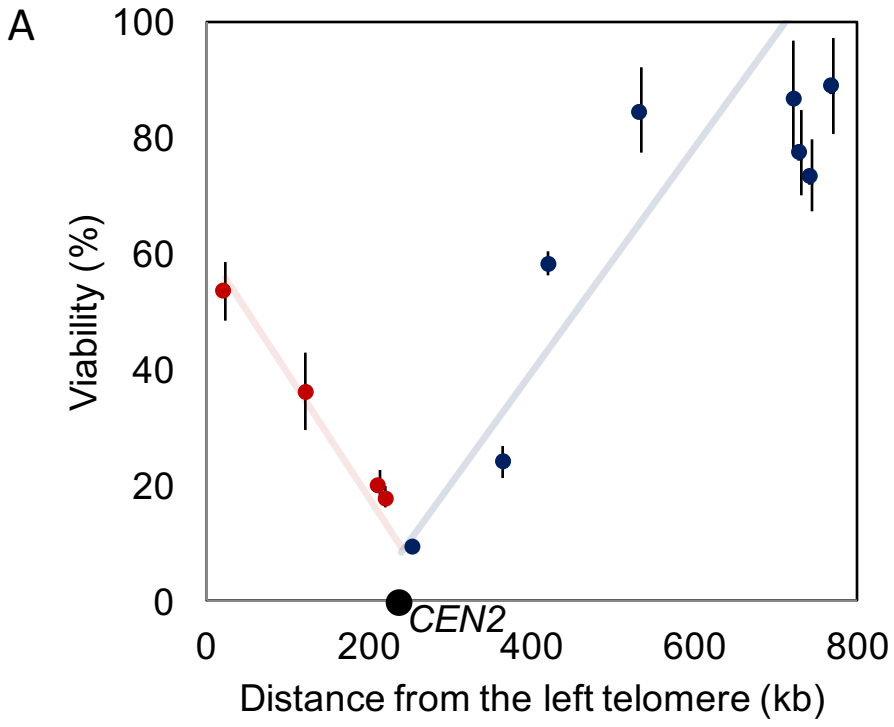


Figure 2

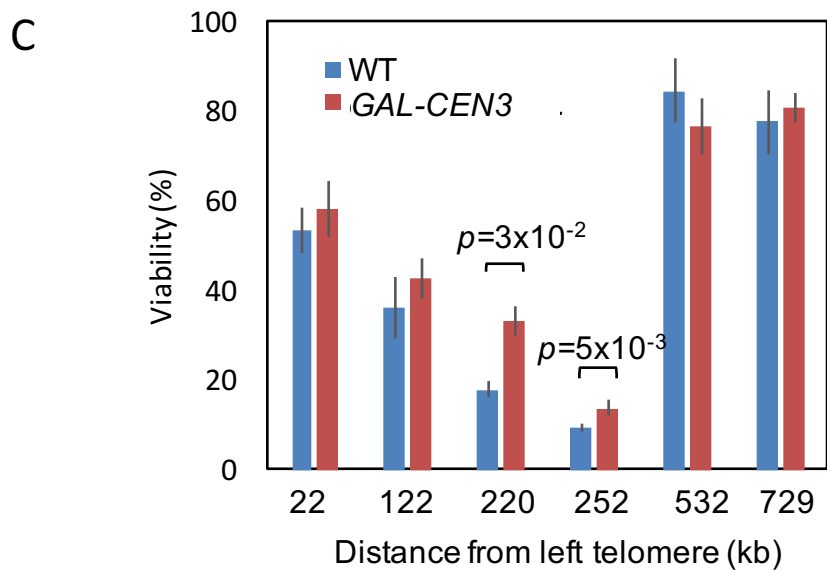
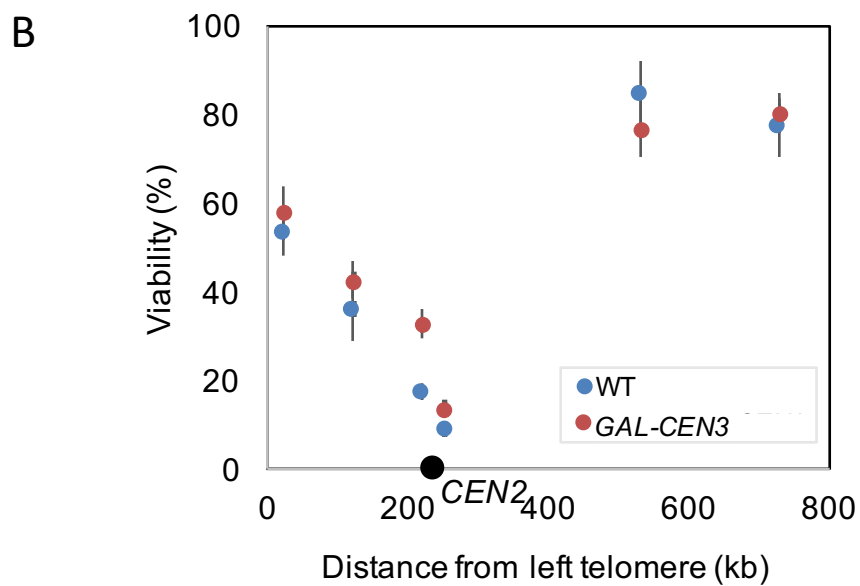
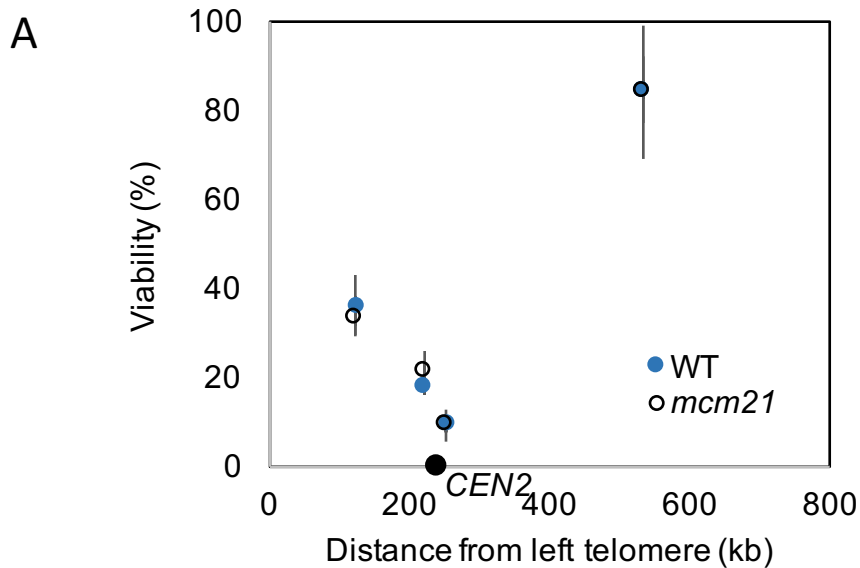
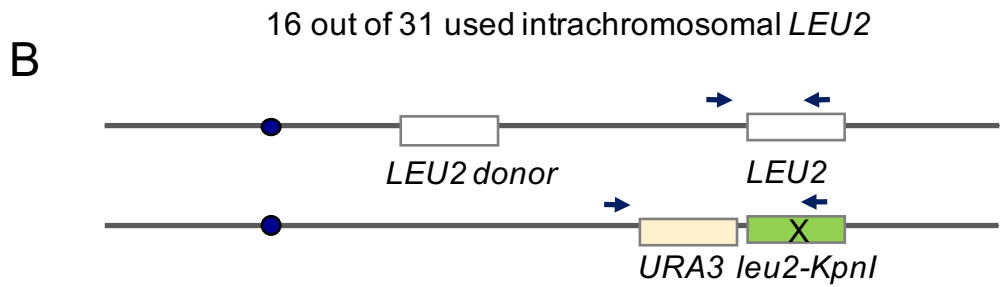
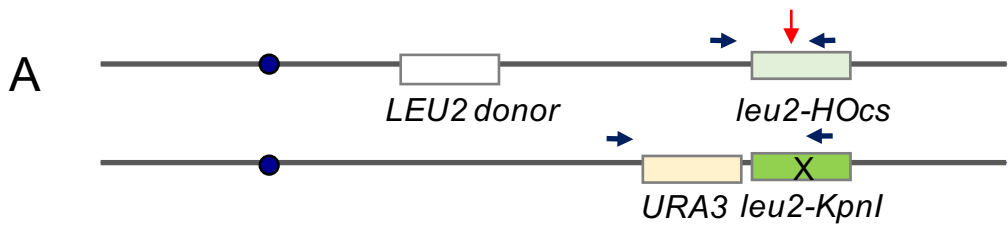
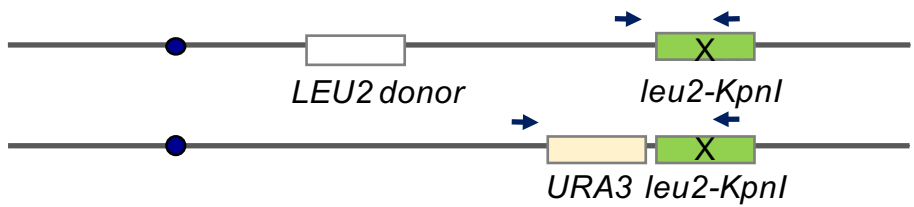


Figure 3



12 out of 31 used *leu2-Kpn1* on homologous chromosome



3 out of 31 used *URA3-leu2-Kpn1* on homologous chromosome

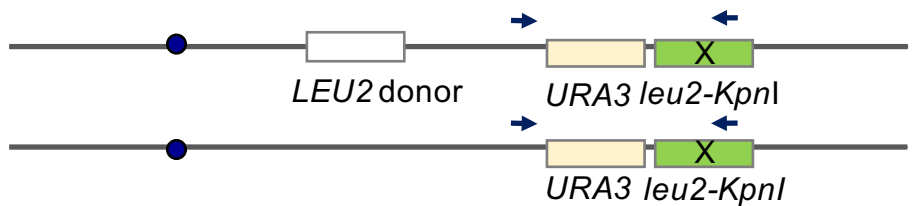


Figure 4